

ES&H Risk Factors from “Interim Storage” of SNF at the Beach: The San Onofre NPP

Subrata Chakraborty^{1*} and Thomas English²

¹University of California, San Diego, Department of Chemistry and Biochemistry, La Jolla CA 92093

²Samuel Lawrence Foundation, Drawer F, Del Mar CA 92014

ABSTRACT

The San Onofre Nuclear Power Plant (SO-NPP), located on the Pacific coast halfway between two metropolises- San Diego and Los Angeles, is in the process of being decommissioned. The present plan, permitted by the California Coastal Commission, is for the interim dry storage of the spent nuclear fuel (SNF) on the premises of the plant at the beach front (~100 feet from the ocean). The SNF is being transferred into 75 thin-walled (1.59 cm (5/8-inch)-thick) Holtec stainless steel canisters and will be essentially buried underground after inserting each of these canisters inside a concrete cavity enclosure container. The nuclear waste might stay there for many decades until the Federal authorities authorize national sites for either interim storage and/or final disposal. In this paper, we are scientifically investigating the potential risk factors associated with storage of SNF as a case study this paper describes those factors that should be considered when estimating risk. We gauge the potential environmental impact of an accident on 8.5 million residents within 50 miles of the NPP.

INTRODUCTION

The San Onofre Nuclear Power Plant (SO-NPP), located on the Pacific coast halfway between two big metropolises- San Diego (population 3.3 million) and Los Angeles population 13.1 million, is in the process of being decommissioned. The present plan, permitted by the California Coastal Commission, is for the interim dry storage of the spent nuclear fuel (SNF) on the premises of the plant at the beach front. The estimated amount of nuclear waste to be processed into the dry storage is about 1,100 tons. There are several radioisotopes of interest with different half-lives: Cs-134 ($t_{1/2} = 2$ years), Cs-137 ($t_{1/2} = 30$ years), Sr-90 ($t_{1/2} = 29$ years), Pu-239/240 ($t_{1/2} = 24,000$ years, 6500 years), I-129 ($t_{1/2} = 16$ million years), I-131 ($t_{1/2} = 8$ days). In an accident, if the radioisotopes are released to the atmosphere (airborne) quick evacuation of the vicinity of the accident site is the only way to shield people from acute exposure from the short half-lived species, but the species with longer lifetimes are the ones which contaminate the soils, waterways, and oceans for a longer period of time, are carried long distances and get incorporated in the food chain [1-8]. Approximately 43% of the intermediate and long-lived radioactivity in the SNL is Cs-137. The reactors at SO-NPP have generated about 7,400 PBq of Cs-137. By comparison, this quantity is more than 6 times the amount released by all atmospheric nuclear weapons tests, and about 89 times that released by the Chernobyl accident. Within that, about 5,000 PBq are stored in the spent fuel pools of SO-NPP and are being transferred to dry cask storage. Each of the storage casks contains about 70 PBq of Cs-137. The recent Fukushima Daiichi Nuclear Power Plant (FD-NPP) accident estimated to release 15-20 PBq of Cs-137, thus each of the casks of SO-NPP are 3 to 4 times more active (with respect to Cs-137) than that released by FD-NPP [3, 5, 8].

In this article, we are investigating the potential risk factors towards an accident from dry storage of SNF in the marine environment. We identify every contributing factor and semi-empirically weigh their risk in the following sections.

POTENTIAL ISSUES OF CONCERN

Performance of Dry Casks

Dry cask storing is a growing method of storing SNF. There is no international standard for the cask design. While most of Europe uses thick (≥ 60 cm) iron casks, thin (1.59 cm) stainless steel (grade 316) designs are being used in the United States (Holtec, Hi-Storm^{TMa} is one such module being used in SO-NPP). Once loaded with dry SNF (fuel rods with cladding), the container lids are welded shut and filled with He (2 atm pressure) and placed inside a concrete enclosure (UMAXTM hole).

Since physical inspection is not an option, there are several model studies to understand the performance of these dry casks, especially the thermal analysis through fluid dynamics [9-11]. Though these SNFs were cooled inside the pool for five years, they are still extremely hot and produce significant amount of heat (heat-load threshold of each canister about 25 – 30 kW) and the threshold temperature of the internal fuel assemblage is 673K (regulatory limit) and the maximum outside temperature is above 450K (with a spatial distribution). Leakage of helium from the canister is one of the safety concerns because that would not dissipate the heat to the wall efficiently and the overall temperature will rise and reach the threshold. One of these studies show that in a scenario with a fuel canister having a heat-load of 30 kW, the time to achieve the thermal limit takes between half a day (fast pressure loss) and one week (slow pressure loss). A decay heat reduction of just a 15% extends the time to go over the thermal threshold to a few weeks. A canister with a decay heat load below 20 kW would never go over the thermal limit set by the regulation.

Helium (He) leakage can happen through failed weld joints or cracks in the canister. The cracks could develop in different ways - via corrosion from enlargement of preexisting scratches and gouges (described in the section below), stress cracking, and metal fatigue to name a few. Being at high temperature, the canisters are always under thermal stress, which is known to produce metal fatigue and can lead to canister rupture in even semi-extreme conditions. Moreover, there is a possibility of material damage in a radiative environment. A study by Nilsson shows that when water (if the SNFs are not dried adequately before loading) is exposed to ionizing radiation, it decomposes into several reactive species (water radiolysis): •OH, H₂O₂, O₂, H₂, H, which can interact with its surroundings [12]. The steady-state concentrations of these species have been shown to drive the corrosion behavior of several materials, including stainless steel. This type of corrosion would start from the inner surface of the canister. There are several studies regarding the corrosion of stainless steel by sea water (chlorine induced) [13-15] (biofilm is another corrosion initiator in marine environment). These studies show a significant possibility of corrosion in stainless steel. The most obvious forms of corrosion of stainless steel in seawater are crevice and pitted corrosion. Crevice corrosion occurs at locations where there is a contact between two identical materials or between a metal and non-metal (deposits, macroscopic biological materials). Pitting occurs without any contact with another material. Both forms of corrosion can be caused by the presence of chloride ions in a solution and are also influenced by temperature and oxidation strength of the solution (e.g., chlorination). A typical electrochemical phenomenon in pitting corrosion is the existence of pitting potential. If, due to external factors, the corrosion potential of the stainless-steel increases above the pitting potential, pitting will occur. The potential corrosion of stainless-steel canisters of SO-NPP could happen because of the presence of marine (chlorinated) air in the ventilation system (always in contact)., The seeping of water at the bottom of the canisters is a possibility as they are situated only 45 cm above the current mean high sea level. Future sea level rise might bring the mean high sea level closer to the bottom, as discussed in a later section (e.g., Sea Level Rise, High Tide, and Coastal Aquifers). Once cracks develop in the canisters, those cracks could propagate rather rapidly, as shown through experiments, and the canister might fail in months-time scale [16].

SNF Loading in Dry Casks

The process of downloading Holtec canisters inside the UMAXTM hole is one of the many initial processes in dry casks storing. There was a “near miss” at the SO-NPP on August 3, 2018, which is at present being

^a HI-STORM UMAX is a trademark of Holtec International

investigated by NRC. As workers were lowering one of the 54-ton canisters packed with high-burnup SNF, the canister got caught on the lip of an inner ring (Fig. 1.), hanging by about 0.6 cm. The drop-restraining system was not in place and the canister was about to fall by about 5.5 m. We have examined this “near miss” scenario from a basic physics standpoint. By examining the dropping of the canister in free fall, we have estimated the upper value of the velocity, kinetic energy, and momentum when the canister crashes into the concrete at the bottom of the UMAX™ cavity. The falling canister could hit the concrete floor at a speed of 40 km/hour with the impact force of over 3×10^8 N. This situation is equivalent to that of a fully loaded 18-wheeler truck with a gross weight of 49,000 kg crashing into reinforced concrete at 40 km/hour. This impact could ruin the canister’s cooling system and potentially cause a large radiation release.

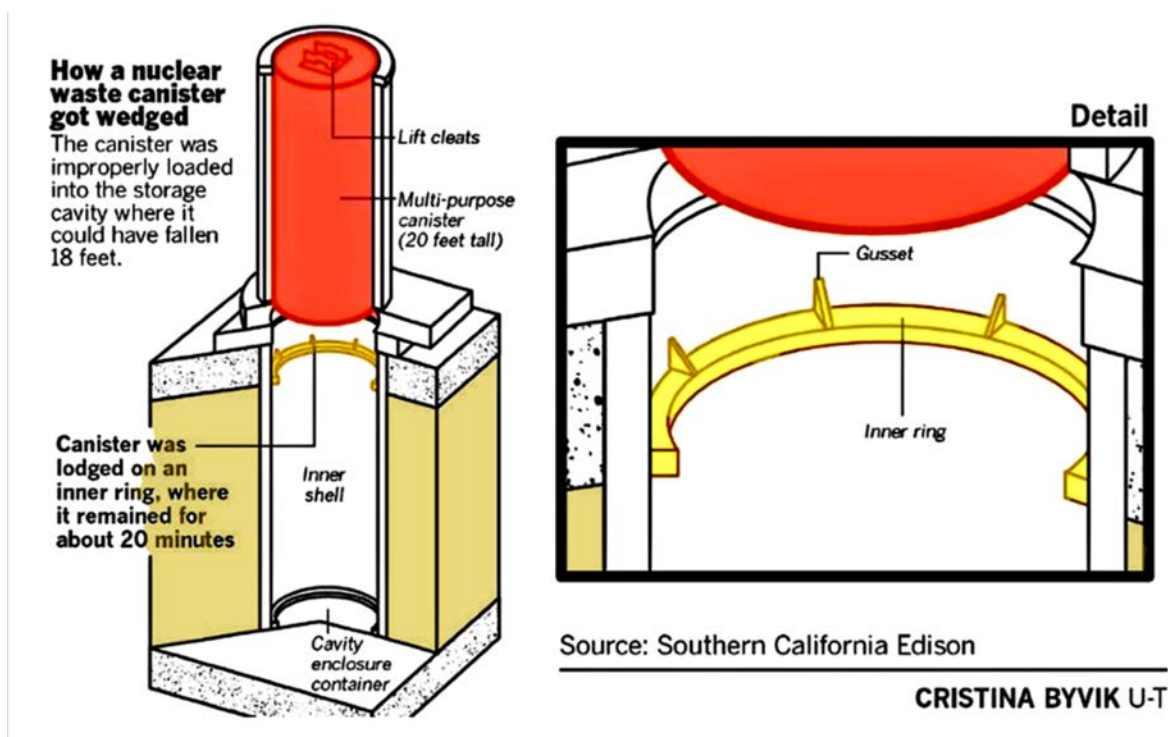


Fig 1. Schematic diagram showing the “near miss” scenario during a downloading process of Holtec canister inside a UMAX™ hole at SO-NPP on August 3, 2018. The graphics credit is as shown in the diagram.

The NRC has previously done an analysis of a similar dropped nuclear waste canister with 1.27-cm walls which are slightly thinner than that used at SO-NPP [17]. This computer simulation included a 6-m drop of the canister from the transfer cask onto a storage overpack pedestal. The canister failure rate was calculated to be about 28%. Similar calculations needed to be performed for SO-NPP to determine if the currently-used system has such a catastrophically high probability of failure.

We envisioned another scenario during the canister loading process in addition to the catastrophic event described above. Due to a small clearance (~0.6 cm) between the canister and the inner ring (Fig. 1.), even during an apparently normal lowering procedure, there is a high probability that the canister will develop gouging and scratching along the vertical direction and will remain undetected. Fig. 2. shows the depth of the scratches (and gouges) based on the size of the load and the size of the intender. The calculation shows (Fig. 2.) that at a 30 % load (weight of canister), an intender of only 6 mm could make a scratch of 15 mm, the thickness of the canister. These calculations must include the effects of the gouging and scratching that

result from both the routine loading of the canisters into the UMAX™ cavity and the gouging and scratching that are associated with a falling canister.

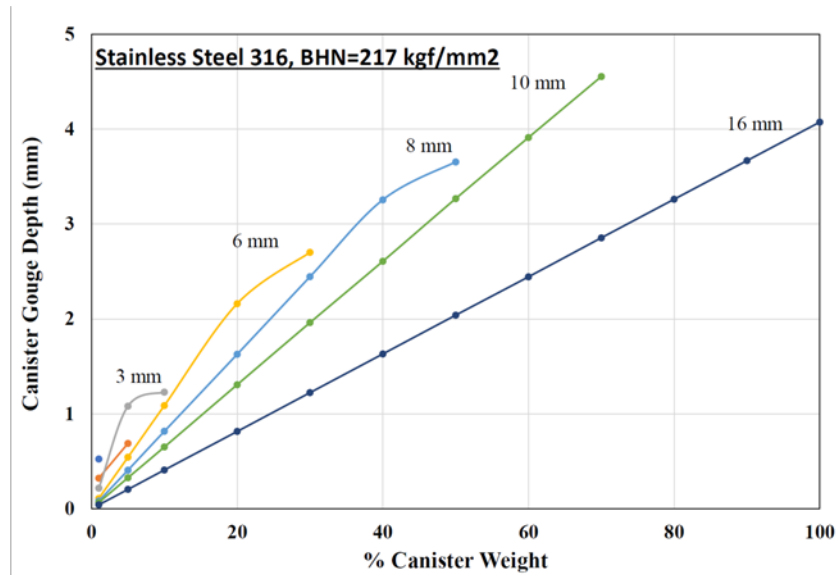


Fig. 2. Calculated penetration depth of scratch or gouge as a function of load for different indenter diameter. The hardness number in Brinell scale for stainless steel 316 (BHN) is 217 kgf/mm² and characterizes the indentation hardness of materials through the scale of penetration of an indenter, loaded on a material test-piece.

NATURAL AND ENVIRONMENTAL FACTORS

Geological Setting of the Site and Earthquakes

The SO-NPP was built in a seismically-active zone on the Pacific coast, which is part of active Pacific-North America transform plate boundaries, and where the seafloor is deformed by several large oblique-slip fault systems [18]. The offshore Southern California Borderland has undergone dramatic adjustments as conditions changed from subduction tectonics to transform tectonics, including major Miocene oblique extension, followed by transpressional fault reactivation. A moderately landward-dipping San Mateo–Carlsbad (SMC) fault converges downward with the steeper, right-lateral Newport-Inglewood/Rose Canyon (NIRC) fault, forming a fault wedge as shown in Fig. 3. near the location of the SO-NPP. The NIRC fault zone is an active strike-slip fault system within the easternmost of the offshore Inner Continental Borderlands (ICB) fault system and an active component of the Pacific-North America plate boundary. NIRC poses a significant hazard to coastal Southern California because of its proximity to some of the most densely populated regions of North America (e.g., San Diego, Orange, and Los Angeles counties as well as Tijuana, Mexico). There are several moderate-sized (magnitude > 5.5 on the Richter Scale) earthquakes in this region in the last 100 years and the estimated epicenters are marked in Fig. 3. [18-20]. Recently, the NIRC fault has been mapped in detail and the rapture magnitudes for three different scenarios are estimated [20]. These authors assigned a magnitude value up to 7.4 for an earthquake from this fault alone without an estimate of the error in this analysis. The prediction of an earthquake is a fascinating area of research, and the prediction of the magnitude is a daunting task. As mentioned, given the wedged-shaped fault system between NIRC and SMC faults, the prediction is more complicated than that from a single fault. In addition to the offshore faults, there are multiple faults east of the SO-NPP. These include the San Jacinto fault and Elsinore fault on the east and the famous San Andreas fault northeast of the SO-NPP. Considering all these

complex geological features together, an earthquake of magnitude ≥ 8 is well within the possibility and could not be ruled out.

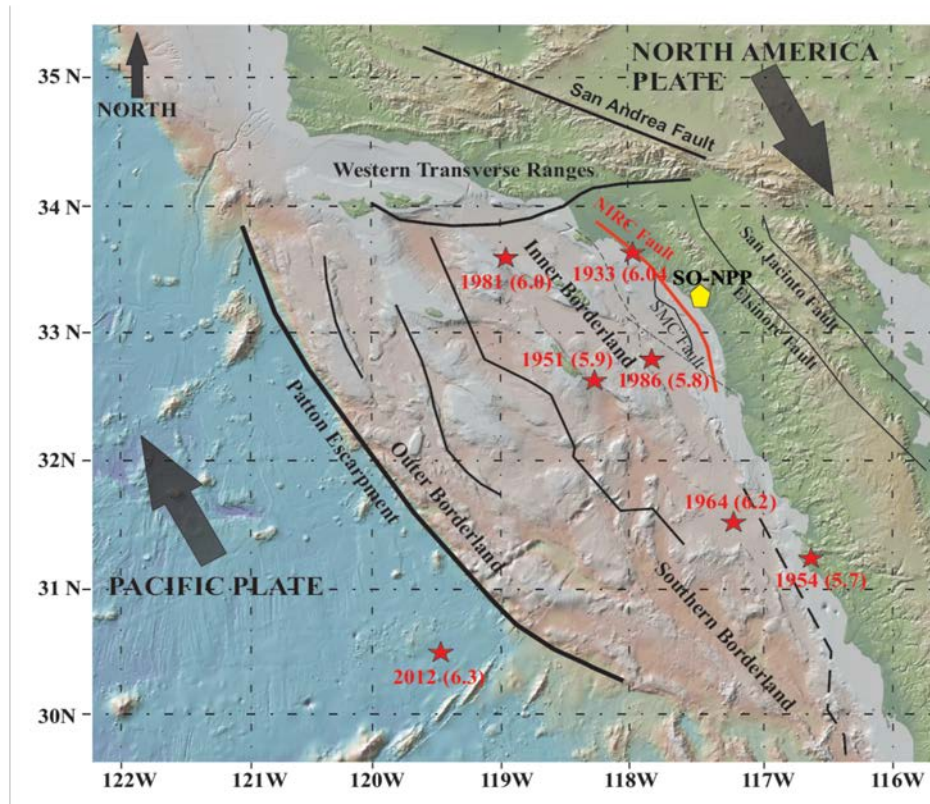


Fig. 3. Geological location map of San Onofre NPP. Data taken from [18-20]. The locations of the epicenters of the previous earthquakes are shown with year of occurrence and magnitude in parenthesis. The location of the faults and the locations of the epicenters of the previous earthquakes are shown for illustration purpose only (and might not be precise). The relative motions of the two plates are also shown. The abbreviations are as mentioned in the text.

Off-Shore Earthquakes and Tsunamis

Tsunamis are the consequence of oceanic earthquakes where long ocean waves sustained by gravity increase in amplitude as water depth decreases. Therefore, such waves are particularly hazardous along populated coastlines near offshore faults that produce a vertical displacement of the seafloor and water column. The hazard from earthquake-generated tsunamis offshore of Southern California has received relatively little attention, however, there is a historical record of tsunamis in this region, two of them within the last 100 years [21]. A recent study [22] updated the possibility of tsunamis in Southern California triggered by an earthquake of magnitude 7.4 in the Ventura Basin (a few tens of miles north of the SO-NPP), which has the similar dip-slip faults as described for the SO-NPP location. With the new studies of the sea floor fault mapping and the computer simulation of the tectonic movements and triggering of a tsunami, we are in a better spot regarding the understanding of the natural hazards present in the region of the SO-NPP. The NRC risk analysis [17] ignored the tsunami risk because of the consideration that the storage sites are far inland, contrary to the SO-NPP location.

Sea Level Rise, High Tide, and Coastal Aquifers

Thermal expansion of the oceans and glacier melting have been the dominant contributors to 20th-century global mean sea level rise. Observations since 1971 indicate that thermal expansion and glaciers (excluding Antarctic glaciers) explain 75% of the observed rise. The contribution of the Greenland and Antarctic ice sheets has increased since the early 1990s, partly from increased outflow induced by warming of the immediately adjacent ocean. Since 1993, when observations of all sea level components are available, the sum of contributions equals the observed global mean sea level rise within uncertainties. Changes in ocean currents, ocean density, and sea level are all tightly coupled such that changes at one location impact local sea level and sea level far from the location of the initial change, including changes in sea level at the coast in response to changes in open-ocean temperature. Although both temperature and salinity changes can contribute significantly to regional sea-level change, only temperature change produces a significant contribution to global average ocean volume change due to thermal expansion or contraction [23].

The global energy balance is a fundamental aspect of the Earth's climate system. At the top of the atmosphere, the boundary of the climate system, the balance involves shortwave radiation received from the Sun, and shortwave radiation reflected, and longwave radiation emitted by the Earth. The rate of storage of energy in the Earth system must be equal to the net downward radiative flux at the top of the atmosphere. This energy imbalance is rising due to increased greenhouse gases in the atmosphere and hence the global increase in temperature. The Intergovernmental Panel on Climate Change (IPCC) adopted a set of emission scenarios known as 'representative concentration pathways', or RCPs. RCPs consist of four future pathways, named for the associated radiative forcing (the globally averaged heat-trapping capacity of the atmosphere measured in watts/square meter) level in 2100 relative to pre-industrial values: RCP 8.5, 6.0, 4.5 and 2.6, respectively. RCP 8.5 is consistent with a future in which there are no significant global efforts to limit or reduce emissions. RCP 2.6 is a stringent emissions reduction scenario and assumes that global greenhouse gas emissions will be significantly curtailed. Under this scenario, global CO₂ emissions decline by about 70% between 2015 and 2050, to zero by 2080, and below zero thereafter. RCP 4.5 and 6 are the two intermediate scenarios and resulted in a similar way.

There is another extreme sea-level rise scenario in the Fourth National Climate Assessment (known as an H++ scenario), which predicts much higher sea level rise in the long run compared to RCP 8.5 [24]. Fig. 4. shows the predicted sea-level rise in different scenarios at La Jolla (several miles south of SO-NPP). By 2030 and 2050, the predicted sea level rise for all the scenarios is similar (around 15 cm by 2030 and 25 cm by 2050), but the predicted rise differs significantly among different scenarios in 2100 and 2150 (Fig. 4.).

Although long-term mean sea-level rise by itself will provoke increasing occurrences of coastal lowlands flooding, over the next several decades it is highly likely that short-term increases in sea level will continue to be the driver of most of the strongest impacts along the coast of California. Short-term processes, including Pacific Basin climate fluctuations (Pacific Decadal Oscillation, El Niño Southern Oscillation, and North Pacific Gyre Oscillation), King tides (perigean high tides), seasonal cycles, and winter storms, will produce significantly higher water levels than sea-level rise alone.

Over the recorded era of the 20th and early 21st centuries, most of the significant storm damage to California's coastline has occurred during major El Niño events, when elevated sea levels coincided with storm waves and high tides. The most prominent of those cases were major El Niño events, for example, 1940-41, 1982-83, and 1997-98, when sea levels were elevated 20-30 cm for several months at a time [25-27].

High tides along the California coast occur twice daily, typically of uneven amplitude, and are caused predominantly by the gravitational attraction of the moon and the sun on the Earth’s oceans. Extreme tides, called spring tides, occur in multi-day clusters twice-monthly at times of the full and new moon. Additionally, even higher tides occur several times a year and are designated as perigean high tides, or more popularly “King tides”. These events are now recognized as producing significant coastal flooding in some well-known areas. The Earth-moon-sun orbital cycles also amplify tidal ranges every 4.4 and 18.6 years, producing peaks in the monthly high tide that are about 15 cm and 8 cm, respectively, higher than in the intervening years [24].

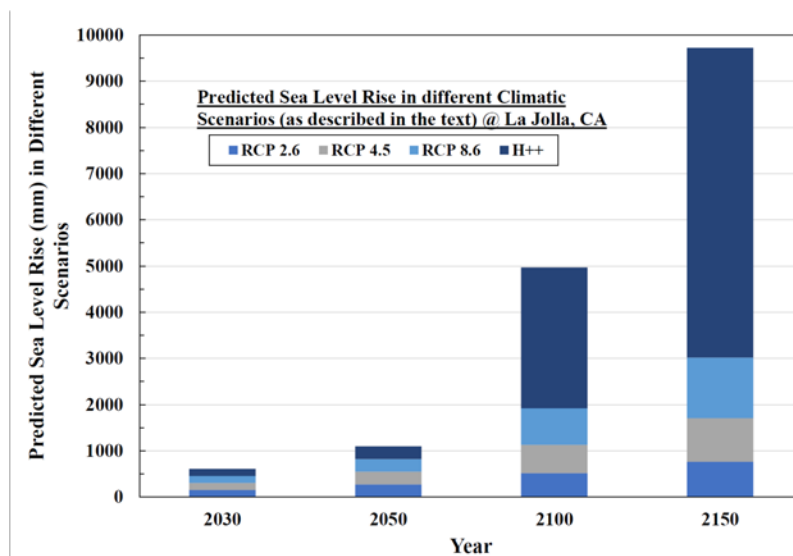


Fig. 4. Predicted sea level rise at La Jolla, CA (several km south of NPP) based on different climatic scenario (emission estimates) described in the text. In all the scenarios the predicted rise is about the same for 2030 and 2050 and diverges thereafter. The plot shows the increases in different scenarios in different shades of blue and are stacked together. The H++ scenario is the extreme case (shown in dark blue) where the predicted sea level increase is dramatic, about 650 cm by 2150 (Data taken from [24]).

Recently, there are several studies addressing the intrusion of seawater in coastal aquifers [28-30] in the context of sea level rise. Sea-level rise related impacts on coastal systems can occur in several ways. Marine inundation will shift the coastline landward, erode beaches, accelerate cliff failure, degrade some coastal habitats, and potentially damage coastal infrastructure. Recent studies have demonstrated that sea level rise also could contribute to saltwater intrusion in coastal regions by raising the interface between intruding saltwater and overlying freshwater.

Sea-level rise and tidal forcing will cause the water table level to rise in the coastal areas, and the mean high sea level could approach and ultimately rise above the ground surface [28]. Moreover, the tides are also known to affect the groundwater fluctuation in the coastal aquifers.

ENVIRONMENTAL FACTORS IN THE CONTEXT OF SNF STORAGE

The SNF from the decommissioning SO-NPP is being buried underground in Holtech thin walled Dry Cask storage encapsulated by concrete barriers. The base of the storage floor is about 45 cm above the mean high sea level. The storage containers are air-cooled through natural diffusion based on in-and-out ventilation. The storage system might withstand a high magnitude earthquake and, at the most, the storage canister might move slightly. But if the earthquake triggers a tsunami, then the risk of canister failure increases significantly. Given a recurrence interval of 1 in 200 years for such a great tsunami, the probability of

occurrence of such an event in the next 30 years is 14% (i.e., $(1-1/200)^{30}$). The huge tsunami waves carry sands and debris onshore in high velocity. The SNF burial ground is protected by a seawall, however, close inspection of the wall indicates inadequate protection from such humongous waves. There is a significant chance of clogging one of the two vents (inlet duct or outlet vent) of each canister by tsunami-carried debris. There are modeling studies to evaluate the dry cask cooling/ventilation system, one of which shows that clogging the outlet vents is more crucial than clogging the inlet vents and without the proper cooling, the fuel temperature might rise above the threshold point (~ 673 K) degrading the cladding, which is known to initiate an explosion [9]. If the probability of clogging one of the vents in an event is 1%, then the chance that one of the 150 total vents (2-vents for each canister with a total of 75 canisters) will clog in such an event is 78% (i.e., $1 - (0.99^{150})$) [this chance reduces to 53% if we reduce the probability of occurrence to 1/2% from 1%]. The tsunami followed by clogging are dependent events and thus the combined chance of such an event is about 11% in a 30-year period.

The sea level rise, the rise of tide levels and the associated rise in the coastal aquifer water level are all interlinked, as discussed. And these climate-related phenomena are related to the storage of SNFs. As the mean high sea level rises in the aquifers, mostly as salt water, the possibility of water seepage (through microcracks in concrete) to the bottom of the canister increases the possibility of corrosion of the stainless-steel canister as discussed earlier. We haven't assigned a probabilistic number to this possibility.

POTENTIAL CONSEQUENCES OF FALLOUT

After Fukushima Accident

The nuclear disaster at FD-NPP followed by the Tohoku earthquake and tsunami on March 11, 2011, led to extensive releases of radioactive gases, volatiles, and liquids, particularly to the coastal ocean due to the power-loss and overheating of the core at the nuclear power plants. This accident provided a unique scientific opportunity to understand the nature and characteristics of the radiation fallout, residence time in soil and vegetation, spreading of radioactivity through ocean circulation and human health [1-6, 8]. Prior to the initial FD-NPP release in 2011, fission radionuclides such as Cs-137 and Sr-90 were detectable worldwide in the food chain, mainly because of fallout from past nuclear weapons tests. Public exposure to naturally occurring radionuclides in food comes largely from K-40 and radionuclides in the U and Th series, contributing approximately 0.3 mSv/year. The total dose varies globally and ranges from 0.2 to 1 mSv/year. Although there have been no direct casualties attributed to radiation exposure, more than 15,000 died or went missing because of the tsunami and earthquake. However, the societal impacts of a nuclear event go far beyond the direct radiological impacts [3], as the area becomes uninhabitable for a longer period of time and severely affects the livelihood of the residence. Here we want to point out that the nuclear disaster from NPP failure is different from that of SNF storage failure. However, we are reviewing the consequences of radiation exposure.

There are four different ways artificial radionuclides ended up in the ocean after the FD-NPP accident: (i) atmospheric fallout (in a period of weeks after the disaster, peaking at 15PBq during mid-March, 2011), (ii) direct discharge to the ocean (in a period of months after the disaster, peaking at 5PBq during early-April, 2011), (iii) groundwater discharge (years after the disaster, 15-20 TBq/year), and (iv) river run-off (years after the disaster, 10-12 TBq/year) [3]. Estimates of the total discharges of Cs-137, the most widely studied radionuclide, have varied from 3 to 30 PBq, but recent and more precise estimates tend to converge on a range of 15-20 PBq.

The monitoring of Fukushima radioactivity is simplified by the fact that the initial Cs-134/Cs-137 activity ratio was about 1 due to the short half-life ($T_{1/2} = 2.1$ year), any residual Cs-134 from nuclear weapon testing was decayed in comparison to Cs-137 ($T_{1/2} = 30$ year).

The radioactivity plume from FD-NPP dissipated rapidly in the energetic coastal waters off Japan under the influence of jet-like currents, tidal currents, and mesoscale eddies, but a significant remnant was transported eastward and reached North America and diverted by northward-flowing Alaskan currents and southward-flowing Californian currents [3, 5, 6, 8]. These discharges from the FD-NPP represent about 25% of the total input of 69 PBq delivered to the North Pacific in the 1950s and 1960s by the nuclear weapon tests, and increased the radiocesium concentration to $\sim 8 \text{ Bq/m}^3$ from the background level of about $1.2\text{--}1.8 \text{ Bq/m}^3$ in surface seawater in the northeastern Pacific [1].

In terms of other radionuclides of the greatest health concern with half-lives of more than 1 year, Sr-90, Pu-239, Pu-240, and I-129 are of interest for longer-term effect. Levels of Sr-90 from the FD-NPPs in atmospheric fallout were, at most, four orders of magnitude lower than Cs-137 measured on land due to its low volatility. Most of the Sr-90 released from the FD-NPPs was directly discharged to the North Pacific, with estimates of total inventories ranging from 0.04 to 1.0 PBq.

Once released to the environment, radionuclides can be rapidly incorporated into marine organisms, either by uptake from seawater, or by food ingestion. Just after the accident, the Japanese authorities had begun conducting gamma analyses of marine organisms for radioprotection purposes and publicly reported several thousand results on the government websites. Cesium is most often measured in the edible part of fish, because Cs, like K, is enriched in fish flesh, which is the largest component of fish body weight, and provides a good estimate of total Cs. In the weeks following the accident, relatively high Cs activities of up to several hundred thousand Bq/kg wet weight (ww) were found in some species of fish caught in the coastal waters of the Fukushima NPP, although the vast majority had activities of less than 1,000 Bq/kg-ww. Occasionally, extremely high values of Cs activity were measured ($>25,000 \text{ Bq/kg-ww}$). Interestingly, the Cs activity values at a given period are not constant over different species (depending on the concentration factor), there are some species for which the activity remained higher ($> 5,000 \text{ Bq/kg-ww}$) even after five years. Sr-90 was also released during the FD-NPP accident and would be expected to accumulate in fish bones, given its geochemical similarity to calcium. However, because the initial ocean activities of Sr were much lower than those of Cs-137, the concentration factors for Sr in marine biota are extremely lower. The measured values of Sr-90 in marine biota were slightly higher than the pre-accident values.

An international assessment was conducted for marine biota under the United Nations Scientific Committee on the Effects of Atomic Radiation [7] based on the monitoring data collected between May 2011 and August 2012 and taking into account two time-stages: an acute exposure phase lasting for a few weeks immediately after the FD-NPP releases, and a chronic exposure phase at a lower dose rate lasting for 90 days to 1 year. During the acute phase, the various marine biota dose estimates were far below (or on the same order of magnitude for macroalgae) the ERICA (Environmental Risk from Ionizing Contaminants: Assessment and Management) acute benchmark value of approximately 5 Gy, which is of concern for marine biota. During the second phase, the weighted absorbed dose rates (Cs-134, Cs-137, and I-131) were highly variable depending on location but were also well below the 0.24 mGy/day ERICA benchmark for chronic exposure (below which no effects are expected at the population level). However, in the FD-NPP harbor, this benchmark was reached and continued to be exceeded even 3 years after the initial FD-NPP release for various species. In the open ocean, very low Cs dose rates were received by planktonic populations both within 30 km of the FD-NPPs and beyond (i.e., 30–600 km) [31]. The resident time of the radioactivity was rather short-lived. Two years after the accidents, the Cs-137 activity was measured in vegetables and fruits and found to be under the regulatory level [2, 4].

Short-Term and Long-Term Effect of Radiation Exposure to Humans

Exposure to ionizing radiation arises from naturally occurring sources (such as radiation from outer space and radon gas emanating from rocks in the Earth) and from sources with an artificial origin (such as medical diagnostic and therapeutic procedures; radioactive material resulting from nuclear weapons testing; energy

generation, including by means of nuclear power; unplanned events such as the NPP accidents at Chernobyl in 1986 and FD-NPP in 2011; and workplaces where there may be increased exposure to radiation from artificial or naturally occurring sources) [31]. It is well documented that radiation exposure can cause cancer or other health effects. High doses of ionizing radiation clearly produce deleterious consequences in humans, including, but not exclusively, cancer induction; certain tissue reactions (such as skin burns and organ failure) may also occur. At very low radiation doses the situation is much less clear, but the risks of low-dose radiation are of societal importance in relation to issues as varied as screening tests for cancer, the future of nuclear power, occupational radiation exposure, frequent-flyer risks, manned space exploration, and radiological terrorism. Although substantive epidemiological data indicate an increased cancer risk from acute doses exceeding 50 mSv, distributing the dose over time appears to lower the risk. The epidemiological data support an increase in cancer risk from protracted exposures exceeding 100 mSv [32]. There are considerable uncertainties in the risk projections, but radiation safety advisory bodies such as the International Commission on Radiological Protection currently estimate the risk of fatal cancer from radiation exposure to the general population to be 5%/Sv, equivalent to 1 fatal cancer arising per 20,000 people exposed to 1 mSv [33]. Fig. 5. schematically shows the effect of exposure dose in humans in terms of duration of exposure and severity along with measured doses during different nuclear accident events (data related to nuclear accidents taken from Table 3 of [3]).

Case studies were reviewed for five of the world’s high background natural radiation areas, or HBNRAs, which are Ramsar (Iran), Guarapari (Brazil), Orissa and Kerala (in India) and Yangjiang (China)) where radiation dose levels range from 15-20 mSv/year [34, 35]. Residences of these HBNRAs have lived in these areas for generations under these extraordinary radiation fields. Interesting, the researchers have not found any direct correlation of genetic mutation or number of cancer cases to the radiation (these numbers are very close to the respective national average) [34].

A recent study found the evidence of genetic mutation (through whole genome sequencing) in human offspring after parental exposure to the high radiation doses. The parents in this study were soldiers in the German military in the late 1950s to early 1980s, who served in radar units on weapon systems that were emitting high-frequency radiation [36].

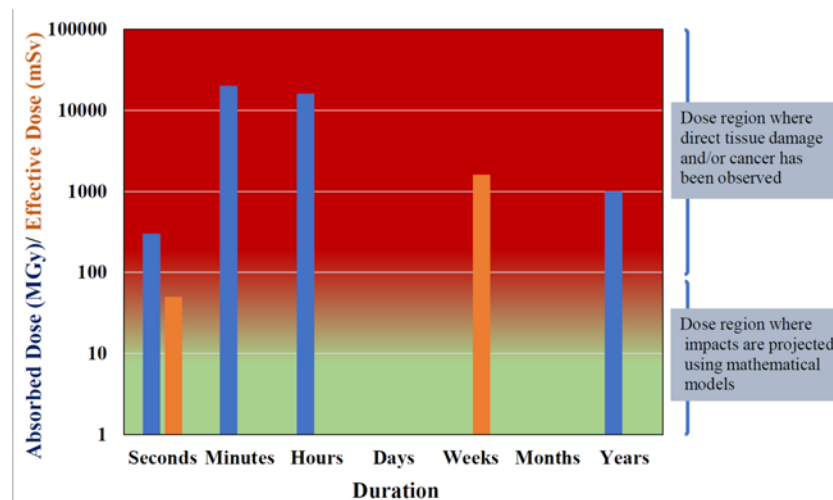


Fig. 5. Schematic showing the effect of radiation doses on human body (Absorbed and Effective doses). The red and green shaded zones indicate different damages as marked. The bars represent various doses measured (absorbed=blue, effective=orange) and the duration of the dose measured during different nuclear accidents (data from [3]).

MONITORING ISSUES WHILE IN STORAGE

Dry cask storage is becoming an increasingly preferred method of storing SNF all over the United States (and World-wide) due to the unavailability of proper long-term geological repository site(s). Due to the intense level of public concern, we decided to investigate the risk involved in such storage in a coastal environment. During the research about this storage method, we discovered that the follow-up monitoring of the dry casks is not standardized, is limited and utterly inadequate. It appears that the dry cask storage is a better option than storing inside the cooling pool for a longer period of time (30+ years, as intermediate storage) [37], however, this prescription does not fit well for all natural settings. As discussed, in the coastal site there are many-fold hazards associated with the storage, including natural and procedural. Therefore, when SNF is stored in coastal environments, effective and proactive monitoring is a must. During the last few years, the volume of research indicates that the scientific community has recognized the need for a better monitoring technique [38-41]. The NRC spectacularly documented the available technique for monitoring temperature, humidity, pressure, chloride, microbial activity, Welded Canister Stress, Corrosion Cracking, Concrete Overpack/Horizontal Storage Module Mechanical and Environmental Degradation, Bolts of Direct-Load Bolted Cask Corrosion, Stress Corrosion Cracking, and Mechanical Degradation of cladding and other internal components (Table ES-1 through ES-4 of [38]. This table indicated the state of monitoring techniques (proposed, tested in the laboratory, or employed in the field), and strengths and weaknesses of each. We presume that is the best starting point for the evaluation of potential risk.

The corruptions on the outer surface of the canisters due to harsh oceanic environment [15], corrosion due to biofilm formation, cracking initiated by scratches and cracks developed during the loading phase (of the canister inside concrete enclosure), are invisible threats carrying significant risk in degradation of the stainless steel and leading to an accident. Deployment of active monitoring is the only way to ensure the safety of the dry cask during storage, for whatever period that may be. Early detection of degradation might provide the required information to the operators to manage the risk involved with the situation. A swift action contingency plan should be in place following monitoring of tsunami-like natural disasters. The clogging of the vents would provide less than 24 hours to control the situation, therefore, continuous temperature monitoring is the most important parameter, which is much easier for the conventional thick containers, compared to the thin ones used at SO-NPP. At present, the SO-NPP storage cask monitoring plan is not available for public review. The SO-NPP plant operator, Southern California Edison (SCE) presently monitors the activity levels around the old storage casks (loaded prior to the decommissioning process) on a monthly basis (personal communication). Without the proper detection of probable failure of the integrity of the canisters, the assessed risk in the storage is extremely high as discussed in the following section, which implies strict age management requirements.

OVERALL RISK ESTIMATION, SHORTCOMING OF ESTIMATION METHODS, QUALITATIVE ASSESSMENT

The risk tree analysis is the preferred method of analyzing risk in the nuclear industry while assessing the risk of dry SNF transportation and storage [17, 42, 43]. The NRC uses the risk triplet, in which the elements of risk are the scenarios, the frequencies of the scenarios, and the consequences of the scenarios, where the measure of risk is the consequences multiplied by the frequency of the consequences [17] and mathematically defined as shown in Eq. 1.

$$R = f \sum_{n=1}^m P_n K_n \dots\dots\dots \text{(Eq. 1)}$$

where R = total risk, f = frequency (1/time), P = conditional probability of the n^{th} accident scenario, and K = consequence of the n^{th} accident scenario. The risk of all plausible accident scenarios in all stages of the dry cask storage operation can also be derived in the same way.

Some of the recent literature followed the similar risk-free analysis and found negligible risk in the entire process [42, 43]. Because of the multiplicative nature, the overall risk of failure of the dry cask storage comes out to be negligibly small and needs additional attention towards the analysis. This kind of analysis does not consider any risk related to the degradation of the canister [17].

Another method for performing risk analysis is through failure mode and risk analysis framework [44], which is a semi-quantitative method. In this type of analysis, every stage of the process could be evaluated separately by determining the Risk Probability Number (RPN). RPN is obtained by multiplying three different factors for every stage: Severity, Occurrence, and Detection. The three factors are ranked on a scale of 1 to 10. For severity, 10 is extreme; for occurrence 10 means the high frequency of occurrence and for detection, 1 means low risk due to high detection ability, and 10 means high risk due to low detection probability. The method is semi-quantitative because, for most cases, the number (scale factor) assigned is subjective (intelligent guess based on some prior experience), however, it identifies processes of different risk levels. The higher the RPN number, the higher is the risk of catastrophe. As an example, Table I shows estimated RPN values for SNF loading and storage in the marine environment.

TABLE I. Failure Mode and Risk Analysis for SNF Loading and Storage in Marine Environment

Stage	Function or Process Step	Failure Type	Potential Impact	SEV (Severity, in scale of 1 to 10)	Potential Causes	OCC (Occurrence, in scale of 1 to 10)	Detection Mode	DET (Detection, in scale of 1 to 10)	Risk Priority Number (RPN=SEV x OCC x DET)
Loading	Dropping	Various (see text)	Explosion triggered by dropping	8	See text	1	Monitoring	1	8
	Scratching	Various (see text)	Scratch due to improper loading	7	See text	2	Monitoring	8	112
Storage In Marine Environment	Corrosion	Various (see text)	Radiation Leakage	10	See text	2	Monitoring	8	160
	Stress cracking	Various (see text)	Radiation Leakage	10	See text	2	Monitoring	8	160
	Earthquake	Various (see text)	Radiation Leakage	5	See text	5	Monitoring	6	150
	Tsunami	Various (see text)	Radiation Leakage	10	See text	2	Monitoring	9	180
	Intentional (Terrorist Attack)/ Unintentional event (Accident)	Various (see text)	Radiation Leakage	10	See text	1	Monitoring	9	90

The risk analysis by these two methods described here yield different outcomes. As an example, during an incident like dropping a canister during transfer, the risk tree analysis identifies as the high-risk process [17, 42, 43], but the failure mode and risk analysis identifies as one of the low-risk ones, because the detection risk is very low (well-trained personnel could easily detect it without any technological aids). When using this analysis for the SO-NPP, tsunamis, followed by the internal degradation of the canister by different processes (as described), was identified as one of the greatest risks because the detection of risk is high for these situations. Although the risk estimation methods are subjective, they are important as they provide a semi-quantitative guideline for mitigating risk factors in SNF handling and storage.

CONCLUSIONS

In this article, we have investigated the potential risk factors for storing SNF in dry cask storage in the beachfront of SO-NPP. The corrosion of the stainless-steel canister, heat dissipation, geological settings and the possibility of tsunamis are discussed. We also discussed the findings after the fall-out of FD-NPP and radiation effect on humans. Finally, we reviewed the usual risk assessment methods and discussed the semi-quantitative failure mode risk analysis to identify the greatest risk among the processes involved. According to our knowledge, SCE has not outlined a detailed monitoring plan after the fuel loadings are done, and at present, their monitoring (of the previous casks) methods are inadequate based on the potential risk areas. Owing to the fact of inadequate monitoring of the storage units, the risk analysis identified storing SNF without proper monitoring (using the available techniques) as the greater risk during exotic events like tsunamis and degradation of the canisters due to harsh coastal air. A strict age management plan with constant monitoring is needed to be in place during the decommissioning phase and prior to storage.

ACKNOWLEDGMENT

We wish to thank Prof. Mark Thiemens (UC, San Diego) and Mr. Rich Drewlowe for their help in doing the research described in this paper. This research has been conducted without any financial support from any agency, institution or person. SC thanks Samuel Lawrence Foundation (of Del Mar CA 92014) for providing the financial support towards the logistics to present this paper in WM Symposium.

REFERENCES

1. J. N. Smith, V. Rossi, K.O. Buesseler, J.T. Cullen, J. Cornett, R. Nelson, A.M. Macdonald, M. Robert and J. Kellogg, "Recent Transport History of Fukushima Radioactivity in the Northeast Pacific Ocean," *Environmental Science & Technology*, 51 10494 (2017).
2. M. Orita, K. Nakashima, Y. Taira, T. Fukuda, Y. Fukushima, T. Kudo, Y. Endo, S. Yamashita, and N. Takamura, "Radiocesium concentrations in wild mushrooms after the accident at the Fukushima Daiichi Nuclear Power Station: Follow-up study in Kawauchi village," *Scientific Reports*, 7, 6744 (2017).
3. K. Buesseler, M. Dai, M. Aoyama, C. Benitez-Nelson, S. Charmasson, K. Higley, V. Maderich, P. Masqué, P.J. Morris, D. Oughton and J.N. Smith, "Fukushima Daiichi–Derived Radionuclides in the Ocean: Transport, Fate, and Impacts," *Annual Review of Marine Science*, 9, 173 (2017).
4. M. Orita, K. Nakashima, N. Hayashida, Y. Endo, S. Yamashita and N. Takamura, "Concentrations of Radiocesium in Local Foods Collected in Kawauchi Village after the Accident at the Fukushima Daiichi Nuclear Power Station," *Scientific Reports*, 6, 28470 (2016).
5. The National Academies Press, "Lessons Learned from the Fukushima Nuclear Accident for Improving Safety and Security of U.S. Nuclear Plants: Phase 2," *National Academies of Sciences, Engineering, and Medicine*, Washington, DC (2016).
6. W. Men, J. He, F. Wang, Y. Wen, Y. Li, J. Huang and X. Yu, "Radioactive status of seawater in the northwest Pacific more than one year after the Fukushima nuclear accident," *Scientific Reports*, 5, 7757 (2015).
7. J. Vives I Batlle, T. Aono, J.E. Brown, A. Hosseini, J. Garnier-Laplace, T. Sazykina, F. Steenhuisen and P. Strand, "The impact of the Fukushima nuclear accident on marine biota: Retrospective assessment of the first year and perspectives," *Science of The Total Environment*, 487, 143 (2014).
8. C. Estournel, E. Bosc, M. Bocquet, C. Ulses, P. Marsaleix, V. Winiarek, I. Osvath, C. Nguyen, T. Duhaut, F. Lyard, H. Michaud and F. Auclair, "Assessment of the amount of cesium-137 released into the Pacific Ocean after the Fukushima accident and analysis of its dispersion in Japanese coastal waters," *Journal of Geophysical Research: Oceans*, 117, C11 (2012).

9. S. Alyokhina, "Thermal analysis of certain accident conditions of dry spent nuclear fuel storage," *Nuclear Engineering and Technology*, 50, 717 (2018).
10. J. Penalva, F. Feria and L.E. Herranz, "Thermal performance of a concrete cask: Methodology to model helium leakage from the steel canister," *Annals of Nuclear Energy*, 108, 229 (2017).
11. S.H. Yoo, H.C. No, H.M. Kim and E.H. Lee, "Full-scope simulation of a dry storage cask using computational fluid dynamics," *Nuclear Engineering and Design*, 240, 4111 (2010).
12. O. Nilsson, "Radiation-induced corrosion of steel," Royal Institute of Technology, Stockholm, Stockholm, 2012.
13. C. Padovani, F. King, C. Lilja, D. Féron, S. Necib, D. Crusset, V. Deydier, N. Diomidis, R. Gaggiano, T. Ahn, P.G. Keech, D.D. Macdonald, H. Asano, N. Smart, D.S. Hall, H. Hänninen, D. Engelberg, J.J. Noël and D.W. Shoesmith, "The corrosion behaviour of candidate container materials for the disposal of high-level waste and spent fuel – a summary of the state of the art and opportunities for synergies in future R&D," *Corrosion Engineering, Science and Technology*, 52, 227 (2017).
14. W. Lv, C. Pan, W. Su, Z. Wang, S. Liu and C. Wang, "Atmospheric corrosion mechanism of 316 stainless steel in simulated marine atmosphere," *Corrosion Engineering, Science and Technology*, 51, 155 (2016).
15. J. Robertson, "The mechanism of high temperature aqueous corrosion of stainless steels," *Corrosion Science*, 32, 443 (1991).
16. A. Iigen, C. Bryan and E. Hardin, Geologic Disposal Requirements Basis for STAD Specification, in: Sandia National Laboratory, U.S. Department of Energy, SAND2015-2175R (2015).
17. A Pilot Probabilistic Risk Assessment Of a Dry Cask Storage System At a Nuclear Power Plant, in: U.S. Nuclear Regulatory Commission, 2007.
18. M.R. Legg, K.M. D., S. Natsumi and S. D. Weeraratne, "High-resolution mapping of two large-scale transpressional fault zones in the California Continental Borderland: Santa Cruz-Catalina Ridge and Ferrello faults," *Journal of Geophysical Research: Earth Surface*, 120, 915 (2015).
19. C.C. Sorlien, J.T. Bennett, M.-H. Cormier, B.A. Campbell, C. Nicholson and R.L. Bauer, "Late Miocene–Quaternary fault evolution and interaction in the southern California Inner Continental Borderland," *Geosphere*, 11, 1111 (2015).
20. V. Sahakian, B. Jayne, D. Neal, H. Alistair, K. Graham and W. Steve, "Seismic constraints on the architecture of the Newport-Inglewood/Rose Canyon fault: Implications for the length and magnitude of future earthquake ruptures," *Journal of Geophysical Research: Solid Earth*, 122, 2085 (2017).
21. J.F. Lander, P.A. Lockridge and M.J. Kozuch, *Tsunamis Affecting the West Coast of the United States 1806–1992, NGDC Key to Geophysical Records Documentation KGRD*, Ed., U.S.D.o. Commer. (Ed.), NOAA, Natl. Geophys. Data Cent., Boulder, Colo., (1993)
22. K.J. Ryan, E.L. Geist, M. Barall and D.D. Oglesby, "Dynamic models of an earthquake and tsunami offshore Ventura, California," *Geophysical Research Letters*, 42, 6599 (2015).
23. J.A. Church, P.U. Clark, A. Cazenave, J.M. Gregory, S. Jevrejeva, A. Levermann, M.A. Merrifield, G.A. Milne, R.S. Nerem, P.D. Nunn, A.J. Payne, W.T. Pfeffer, D. Stammer and A.S. Unnikrishnan, *Climate Change 2013: The Physical Science Basis. Contribution of Working Group I to the Fifth Assessment Report of the Intergovernmental Panel on Climate Change*, Ed., T.F. Stocker, D. Qin, G.-K. Plattner, M. Tignor, S.K. Allen, J. Boschung, A. Nauels, Y. Xia, V. Bex, P.M. Midgley, Cambridge University Press, Cambridge, United Kingdom and New York, NY, USA (2013).
24. G. Griggs, J. Árvai, D. Cayan, R. DeConto, J. Fox, H. Fricker, R. Kopp, C. Tebaldi and E. Whiteman, *Rising Seas in California: An Update on Sea-Level Rise Science*, Ed., C.O.P.C.S.A.T.W. Group, California Ocean Science Trust (2017).
25. S.-W. Yeh, J.-S. Kug, B. Dewitte, M.-H. Kwon, B.P. Kirtman and F.-F. Jin, "El Nino in a changing climate," *Nature*, 461, 511 (2009).
26. J.S.W. J. J. Barsugli, A. F. Loughie and Z.T. P. D. Sardeshmukh, "The effect of the 1997/98 El Nino on individual large-scale weather events," *Bulletin of the American Meteorological Society*, 80, 13 (1999).
27. R.A. Feely, "Distribution of chemical tracers in the eastern equatorial Pacific during and after the 1982-1983 El Nino/Southern Oscillation event," *J. Geophys. Res.*, 92, 6545 (1987).

28. D.J. Hoover, K.O. Odigie, P.W. Swarzenski and P. Barnard, "Sea-level rise and coastal groundwater inundation and shoaling at select sites in California, USA," *Journal of Hydrology: Regional Studies*, 11, 234 (2017).
29. J. Chun, C. Lim, D. Kim and J. Kim, "Assessing Impacts of Climate Change and Sea-Level Rise on Seawater Intrusion in a Coastal Aquifer," *Water*, 10, 357 (2018).
30. C. Singaraja, S. Chidambaram and N. Jacob, "A study on the influence of tides on the water table conditions of the shallow coastal aquifers," *Applied Water Science*, 8, 11 (2018).
31. Report of the United Nations Scientific Committee on the Effects of Atomic Radiation to the General Assembly, Ed., U.N.S.C.o.t.E.o.A. Radiation, United Nations, New York (2017).
32. D.J. Brenner, R. Doll, D.T. Goodhead, E.J. Hall, C.E. Land, J.B. Little, J.H. Lubin, D.L. Preston, R.J. Preston, J.S. Puskin, E. Ron, R.K. Sachs, J.M. Samet, R.B. Setlow and M. Zaider, "Cancer risks attributable to low doses of ionizing radiation: Assessing what we really know," *Proceedings of the National Academy of Sciences*, 100, 13761 (2003).
33. The 2007 Recommendations of the International Commission on Radiological Protection ICRP Publication 103 (2007).
34. A.S. Aliyu and A.T. Ramli, "The world's high background natural radiation areas (HBNRAs) revisited: A broad overview of the dosimetric, epidemiological and radiobiological issues," *Radiation Measurements*, 73, 51 (2015).
35. V. Jain, P.R.V. Kumar, P.K.M. Koya, G. Jaikrishan and B. Das, "Lack of increased DNA double-strand breaks in peripheral blood mononuclear cells of individuals from high level natural radiation areas of Kerala coast in India," *Mutation Research/Fundamental and Molecular Mechanisms of Mutagenesis*, 788, 50 (2016).
36. M. Holtgrewe, A. Knaus, G. Hildebrand, J.-T. Pantel, M.R.d.l. Santos, K. Neveling, J. Goldmann, M. Schubach, M. Jäger, M. Coutelier, S. Mundlos, D. Beule, K. Sperling and P.M. Krawitz, "Multisite de novo mutations in human offspring after paternal exposure to ionizing radiation," *Scientific Reports*, 8, 14611 (2018).
37. R. Alvarez, J. Beyea, K. Janberg, J. Kang, E. Lyman, A. Macfarlane, G. Thompson and F.N. von Hippel, "Reducing the Hazards from Stored Spent Power-Reactor Fuel in the United States," *Science & Global Security*, 11, 1 (2003).
38. Available Methods for Functional Monitorin of Dry Cask Storage Systems, Ed., U.S.Nuclear Regulatory Commission, Contract-NRC-HQ-12-C-02-0089 (2014).
39. S. Choi, H. Cho and C.J. Lissenden, "Nondestructive inspection of spent nuclear fuel storage canisters using shear horizontal guided waves," *Nuclear Engineering and Technology*, 50, 890 (2018).
40. R. Meyer, S. Suffield, E. Hirt, J. Suter, J. Lareau, J. Zhuge, A. Qiao, T. Moran and P. Ramuhalli, *Nondestructive Examination Guidance for Dry Storage Casks*, Ed., U.S.D.o. Energy (2016).
41. Dry Cask Storage Inspection and Monitoring, Ed., N.E.D. Argonne National Laboratory (2012).
42. M. Yun, R. Christian, B.G. Kim, B. Almomani, J. Ham, S. Lee and H.G. Kang, "A software tool for integrated risk assessment of spent fuel transportation and storage," *Nuclear Engineering and Technology*, 49, 721 (2017).
43. K.C. Chen, K. Ting, Y.C. Li, Y.Y. Chen, W.K. Cheng, W.C. Chen and C.T. Liu, "A study of the probabilistic risk assessment to the dry storage system of spent nuclear fuel," *International Journal of Pressure Vessels and Piping*, 87, 17 (2010).
44. J. Yang, H.-Z. Huang, L.-P. He, S.-P. Zhu and D. Wen, "Risk evaluation in failure mode and effects analysis of aircraft turbine rotor blades using Dempster–Shafer evidence theory under uncertainty," *Engineering Failure Analysis*, 18, 2084 (2011).